Phys Chem Minerals (1993) 20:19–26

PHYSICS AND CHEMISTRY OF MINERALS

Impedance Spectroscopy of Single and Polycrystalline Olivine: Evidence for Grain Boundary Transport

J.J. Roberts* and J.A. Tyburczy

Department of Geology, Arizona State University, Tempe, AZ 85287-1404, USA

Received June 5, 1992 / Revised, accepted November 2, 1992

Abstract. The impedance spectra of single and polycrystalline olivine display two and three impedance arcs, respectively. Impedance spectra of single crystal olivine, polycrystalline olivine compacts, and natural dunite are compared to deduce the causes of the different impedance arcs. Variation of sample dimensions and use of three- and four-electrode configurations aid in the interpretation. The resistance of the two highest frequency mechanisms varies directly with the length to area ratio (l/A) of the sample. Experiments using the four-electrode configuration confirm that the lowest frequency impedance arc is caused by processes at the sample-electrode interface. In both single and polycrystalline samples the highest frequency mechanism is interpreted as bulk (grain interior) conduction, and the lowest frequency mechanism is attributed to sample-electrode interface effects. In the polycrystalline samples, the intermediate frequency mechanism is interpreted as the grain boundary conduction mechanism. The resistances of the grain interior and grain boundary mechanisms add in a series manner.

Introduction

Grain boundaries are known to play an important role in the diffusive, mechanical, and electrical properties of many polycrystalline materials. Understanding how grain boundaries affect the electrical properties of polycrystalline olivine is important to our interpretation of the lower crust and upper mantle. It is the purpose of this study to demonstrate that polycrystalline olivine displays a different frequency dependent electrical response than single crystal olivine by observing the impedance spectra of 1) ground-and-pressed olivine compacts, 2) dunites, and 3) single crystal olivine. The impedance spectra of these materials exhibit impedance arcs in the complex plane. These arcs represent different conduction mechanisms that are separated in frequency because they have different relaxation times. By performing experiments on samples with different dimensions and using different electrode configurations, it is possible to determine the conduction mechanisms responsible for the individual impedance arcs. In this way information pertaining to the role of grain boundaries on the overall electrical properties of a material may be obtained.

In this work we measure the frequency dependent electrical behavior of polycrystalline and single crystal olivine over the frequency range 10^{-4} to 10^{5} Hz. Several mechanisms having different relaxation times are observed in this extended frequency range. By making 4 to 6 measurements per decade of frequency, the impedance spectra are generally more well-defined and the individual mechanisms are more easily observed than in studies where only 1 to 2 measurements per decade of frequency are reported. Because field measurements are made in this range of frequencies it is important to measure the electrical response of Earth materials over this same frequency range.

In previous papers, Roberts and Tyburczy (1991) and Tyburczy and Roberts (1990) made frequency dependent electrical measurements (10^{-4} to 10^{4} Hz) on ground-and-pressed olivine compacts from 800 to 1400° C. They observed impedance arcs in the complex impedance plane and interpreted them as grain interior, grain boundary, and electrode mechanisms from high to low frequency, respectively. The present work adds to the previous work and provides direct evidence for that interpretation by analyzing experiments comparing single versus polycrystalline olivine, two- versus four-electrode experiments, and experiments with variable sample dimensions.

Nomenclature

Impedance is a complex quantity that includes an ohmic resistance (the real component) and a reactance (the im-

* *Present address:* Lawrence Livermore National Laboratory, P.O. Box 808, L-365, Livermore, CA 94551, USA

aginary component). In this work the impedance is expressed as a magnitude and a phase ($|Z|$, ϕ), and as a real component and an imaginary component (Z', Z''), or as a resistance and a capacitance (R, C). The complex impedance Z^* is given by

$$Z^* = Z' - jZ'' \quad (1)$$

where the asterisk denotes a complex quantity, a single prime indicates a real quantity, the double prime indicates an imaginary quantity, and j is $\sqrt{-1}$. The real and imaginary parts of the impedance are obtained from the measured quantities $|Z|$ and ϕ determined at a given frequency by $Z' = |Z| \cos \phi$, and $Z'' = |Z| \sin \phi$. The complex impedance can also be represented by $Z^* = R - jX_c$, where R corresponds to Z', the reactance $X_c = 1/\omega C$ corresponds to Z'', and ω is the angular frequency.

Previous Work

There are many studies in the ceramics literature that utilize electrical measurements as a function of frequency to determine the electrical properties of grain boundaries (e.g., Bauerle 1969; Verkerk et al. 1982b; van Dijk and Burggraaf 1981). Bauerle (1969) reported the electrical response of polycrystalline yttria stabilized zirconia (YSZ), and employed an equivalent circuit of resistors and capacitors to describe the experimentally observed response. By comparing measurements made with two- and four-electrode configurations, and by examining the variation of the individual circuit parameters with sample dimensions, he concluded that the high, intermediate, and low-frequency responses are due to grain interior (bulk), grain boundary, and electrode processes, respectively. Abelard and Baumard (1980) measured the frequency dependent electrical properties of sintered forsterite over the frequency range 10^{-1} to 10^5 Hz. They observed a frequency dependent electrical response, but did not specifically address the role of grain boundaries in their measurements. Sato et al. (1986) studied the frequency dependent electrical properties of partially molten gabbro. Although Sato et al.'s study does not investigate grain boundary conduction, it does demonstrate that the effects of electrodes are observed at the lowest frequencies of measurement, and that by making a frequency dependent electrical measurement a correction can be made that eliminates the effects of the electrodes from the measurements. Sato (1986) also investigated the frequency dependent electrical properties of single crystal San Carlos olivine over the frequency range 0.1 to 1000 Hz from 1000 to 1400° C as a function of oxygen partial pressure. An important aspect of Sato's study is that different defect species have different relaxation frequencies and information about the different defect species is obtained by measuring the frequency dependence of the dielectric constant.

A contrasting view of the frequency dependence of electrical properties is presented by Constable and Duba (1990) who measured the electrical conductivity of polycrystalline dunite from Jackson County, North Carolina. Between 0.1 and 10 kHz they reported dispersion of conductivity less than 2 hundredths of a log unit. Their lowest frequency of measurement roughly coincides with the frequency of maximum phase angle commonly observed in other frequency dependent measurements (Huebner and Voigt 1988; Roberts and Tyburczy 1991). This could mean that they did not measure the electrical properties at frequencies low enough to observe additional conduction mechanisms. Another important factor is that Constable and Duba measured the impedance magnitude and did not report a phase angle measurement. The frequency variation of electrical measurements is commonly most pronounced in plots of the phase angle versus frequency, the real and imaginary impedances versus frequency, and the imaginary impedance versus the real impedance in the complex plane.

Experimental Procedures

Samples and Sample Preparation

Experiments were performed on ground-and-pressed polycrystalline samples prepared from San Carlos olivine (Fo_{91}) single crystals, a single crystal olivine from San Carlos, Arizona, and natural dunite samples. The ground-and-pressed compacts were prepared according to the procedure described in Roberts and Tyburczy (1991). Two different natural dunite samples were examined. The first natural sample was a dunite from the San Quintin volcanic field in Baja California, Mexico (Basu and Murthy 1977). The San Quintin dunite contains approximately 95% olivine ($Fo_{90.5}$), 3% clinopyroxene and 2% spinel (Roberts and Tyburczy 1991). It is relatively fine-grained with an average grain size of 0.2–0.4 mm. The second natural dunite is from Jackson County, North Carolina. It has an average grain size of 0.4 mm and the olivine is $Fo_{92.5}$ in composition. The samples employed have no serpentine or chlorite alteration.

The single crystal sample was prepared from a large gem quality olivine specimen from San Carlos, Arizona (Fo_{91}). This specimen was oriented optically to within ±3° of the [001] axis and was carefully examined to 500× to insure that it was free of fractures and inclusions.

The method of preparing the samples for electrical properties measurements is described in detail in Roberts and Tyburczy (1991). Significant differences are noted here. Pt electrodes were used for all the experiments except for samples NCD5E, NCD6A, and NCD7A (Table 1) in which Ir electrodes were employed. No difference in the electrical response of the material was observed with the different electrode materials. Loss of Fe to the electrodes was confined to the outermost 25 μm of the sample (or less) and the loss in this outer zone was generally less than 2 wt% Fe. Iron loss was checked for during the experiments by making measurements at a specific frequency at different times during the course of an experiment. The variation in Z' (and $|Z|$) at 100 Hz was less than 5% for experiments lasting 10 to 24 hours. Hirsch and Shankland (1991) present a quantitative defect model of electrical conduction in olivine and conclude that a small loss of Fe to electrodes does not significantly affect electrical conductivity or oxygen diffusivity in olivine.

The electrical measurements were made in a one atmosphere total pressure gas mixing furnace. Samples were allowed to equilibrate to experimental conditions for a period of 4–20 hours depending on sample dimensions, grain size, and the experimental temperature. During equilibration the resistance of the sample was monitored at specific frequencies and gradually reached a steady value. The oxygen fugacity was controlled with a CO/CO_2 mixture and was accurate to within ±0.15 log units as determined by an yttria stabilized zirconia (YSZ) oxygen sensor. Temperatures were

Table 1. Fitting parameters to impedance data using equivalent circuit of Fig. 2

Run name	Temp, °C	f_{O_2}, Pa	A/l, m	R_1, Ω	C_1, F	R_{DE2}, Ω	τ_{DE2}, s	α_{DE2}
Polycrystalline olivine compacts								
PC10	1200	$10^{-5.0}$	0.0424	$2.05\pm0.01\times10^{4}$	n.d.	$2.01\pm0.01\times10^{4}$	$8.66\pm0.12\times10^{-2}$	0.30 ± 0.01
PC6F	1200	$10^{-5.0}$	0.0392	$2.42\pm0.03\times10^{4}$	$2.59\pm0.07\times10^{-10}$	$1.97\pm0.52\times10^{4}$	$1.14\pm0.30\times10^{-1}$	0.44 ± 0.04
PC6G	1200	$10^{-5.0}$	0.0240	$4.18\pm0.03\times10^{4}$	$2.70\pm0.04\times10^{-10}$	$4.58\pm0.08\times10^{4}$	$6.04\pm0.48\times10^{-1}$	0.34 ± 0.01
PAH	1200	$10^{-4.0}$	0.0231	$4.08\pm0.01\times10^{4}$	$6.23\pm0.01\times10^{-10}$	$4.78\pm0.02\times10^{4}$	$4.10\pm0.21\times10^{-1}$	0.55 ± 0.01
North Carolina dunite								
NCD3A	1200	$10^{-4.4}$	0.0553	$3.80\pm0.01\times10^{4}$	$9.67\pm0.24\times10^{-12}$	$1.11\pm0.04\times10^{4}$	$1.16\pm0.13\times10^{-2}$	0.56 ± 0.01
NCD5E	1200	$10^{-4.3}$	0.0172	$9.97\pm0.26\times10^{4}$	$9.81\pm0.77\times10^{-12}$	$6.26\pm0.90\times10^{4}$	$2.77\pm0.85\times10^{-2}$	0.55 ± 0.04
NCD6A	1200	$10^{-4.3}$	0.0115	$1.41\pm0.01\times10^{5}$	$7.11\pm0.13\times10^{-12}$	$9.15\pm0.34\times10^{4}$	$4.85\pm0.37\times10^{-2}$	0.53 ± 0.01
NCD7A	1200	$10^{-4.3}$	0.0175	$1.31\pm0.01\times10^{5}$	$5.20\pm0.12\times10^{-12}$	$3.61\pm0.61\times10^{4}$	$4.19\pm0.59\times10^{-2}$	0.58 ± 0.05
San Carlos single crystal, [001]								
SC23	1198	$10^{-4.3}$	0.0170	$7.18\pm0.28\times10^{4}$	$2.52\pm0.20\times10^{-10}$	$1.25\pm0.04\times10^{5}$	$3.45\pm0.49\times10^{-1}$	0.38 ± 0.01

Grain size ranges for the polycrystalline compacts are: PC10, 7–15; PC6F and PC6G, 35–45; PAH, 75–180 μm. n.d. – not determined

controlled and monitored to ±3° C with Pt 70-Rh 30/Pt 94-Rh 6 thermocouples. The temperature gradient between the top and bottom of the sample was less than 1° C.

An important factor to consider is the state of the grain boundaries: whether or not they are intact, and what effect grain boundary microcracking has on the electrical properties of the grain boundaries. Based on a previous analysis of thermal expansion anisotropy in olivine compacts (Roberts and Tyburczy 1991) and on physical inspection of the samples following an experiment, it can be concluded that at least partial grain-to-grain contact exists in these samples. In many cases sintering during the long duration of an experiment (20–40 hours) increases the overall competency of the sample and presumably the degree of grain-to-grain contact, without significant differences in the observed impedance spectrum. In addition, impedance spectra of ZrO_2 with grain sizes as small as 4 μm are qualitatively similiar to those of this study (Verkerk et al. 1982b). On the other hand, acoustic and mechanical properties indicate that microcracks exist in samples such as these (Kuszyk and Bradt 1973). Clearly, experimentation at elevated pressures is needed to resolve this issue.

Impedance Measurements

Electrical measurements were made over the frequency range 5×10^{-5} to 10^{5} Hz using two data collection systems. Between 5×10^{-5} and 10^{4} Hz data were collected using the system described by Roberts and Tyburczy (1991). At frequencies from 5 to 10^{5} Hz, data were collected with a Hewlett Packard 4192 Impedance Spectrum Analyzer. The two systems overlap in frequency between 0.005–10 kHz (Fig. 1a); between 5–100 Hz measurements of $|Z|$ and ϕ are nearly identical for the two systems. The low-frequency system is limited at high frequencies because of cross-talk between the leads and the frequency response of the instrumentation amplifiers. The high-frequency system has a built in correction to eliminate the effects of stray capacitance at the highest frequencies. The frequency at which we have switched from data obtained using one system to the other for input into the equivalent circuit fitting routine is typically 30–70 Hz. Accuracy of the measuring systems was checked by analyzing circuits of precision resistors and capacitors with values known to within 1%.

Results and Discussion

Experimental Data

A set of impedance measurements typical for polycrystalline olivine is shown in Fig. 1 (1200° C, $f_{O_2}=$

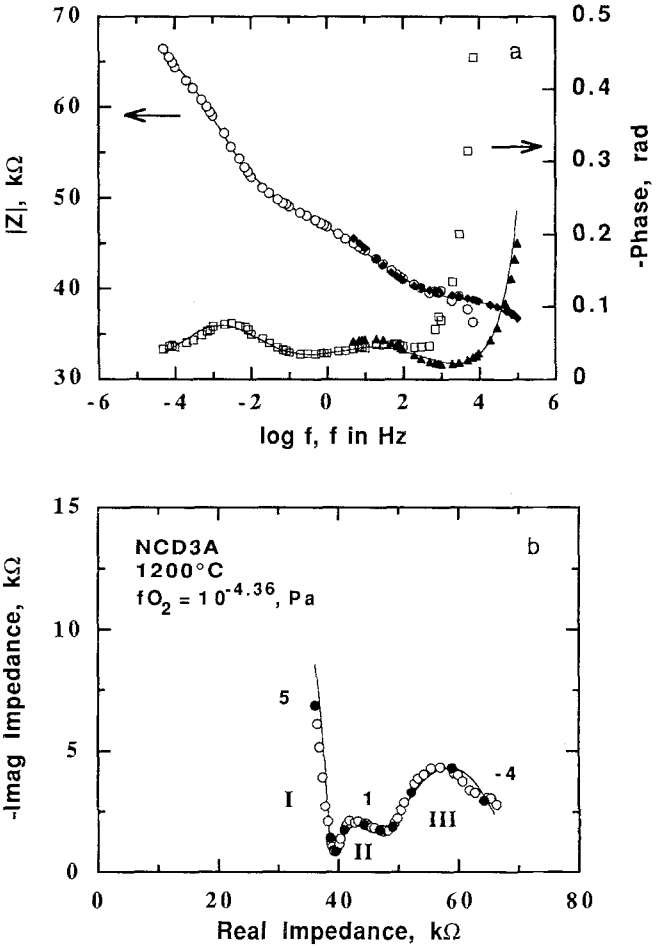

Fig. 1. a, b Impedance data for the North Carolina Dunite collected at 1200° C and an f_{O_2} of $10^{-5.2}$ Pa (Pt electrodes). **a** Impedance magnitude and phase angle versus log frequency in Hz. All data collected by both the high frequency (HF) and low frequency (LF) systems are displayed. Symbols: *open circles*, $|Z|$, LF; *solid diamonds*, $|Z|$, HF; *open squares*, phase angle, LF; *solid triangles*, phase, HF. **b** Complex impedance plane plot of the data. A filled circle occurs every decade of frequency; numerals are log frequency of the corresponding filled data point. The lines through the data are model responses obtained from CNLS fitting with an equivalent circuit

$10^{-5.2}$ Pa, dunite from Jackson County, North Carolina). The measured parameters $|Z|$ and ϕ are plotted against frequency in Fig. 1a. In Fig. 1b, the imaginary part of the complex impedance Z'' is plotted against the real part Z'. The complex impedance plane plot displays parts of three impedance arcs, which are circular arcs approximately centered on the real axis. Each impedance arc has a different characteristic relaxation time ($\tau = R \cdot C$) and corresponds to a separate conduction process that is dominant over a distinct frequency range. Impedance arcs will be distinct in the complex impedance plane if the time constants differ by a factor of about 100 or more. The impedance spectra presented in this paper display two or three impedance arcs occurring at high, intermediate, and low frequency ranges (referred to as arcs I, II, and III, respectively, Fig. 1b). An arc can be partial or incomplete if it extends past the range of measurement or adjacent impedance arcs can overlap.

Modeling the Data with Equivalent Circuits

Each impedance spectrum is modeled using a circuit of resistors, capacitors, and other more specialized circuit elements using a complex non-linear least squares (CNLS) fitting routine described in detail by Macdonald et al. (1982). Values for individual resistors and capacitors are obtained that are then related to specific conduction and polarization mechanisms within the material (Macdonald 1985; Roberts and Tyburczy 1991). Because we observe impedance arcs that have different time constants, i.e., the impedance arcs occur over different ranges of frequency and are distinct on complex impedance plane plots, the equivalent circuit generally consists of two or more parallel RC circuit elements connected in series. A parallel RC element produces a semi-circle in the complex impedance plane, having a center that falls on the real axis. Because in real materials the electrical response often exhibits impedance arcs with centers that lie below the real axis, a constant phase element (CPE) is used in the equivalent circuit in place of the capacitor to empirically account for the depressed impedance arcs. With the use of the CPE an additional parameter α is introduced to the fit corresponding to the angle of depression of the impedance arc. The equation describing the complex impedance of the circuit element containing a CPE and a resistor in parallel (also referred to as a distributed circuit element) ist

$$Z^*_{ZARC} = \frac{R}{1+(j\omega\tau)^{\alpha}} \qquad (2)$$

where $j = \sqrt{-1}$, and $\alpha = 1\text{–}2\,\theta/\pi$. The exponent α varies between 0 and 1, and θ is the angle of depression of the center of the impedance arc below the real axis. For $\alpha = 1$, the CPE is an ideal capacitor. Distributed elements and their responses are discussed by many authors (e.g., Macdonald 1985; Raistrick 1987). Numerous equivalent circuits can be used to describe the frequency response of the impedance data. The general form of the equivalent circuit used to model the results of this study is shown in Fig. 2. This circuit was chosen because it accurately describes the experimentally observed frequency response over the entire frequency range of measurement, yet is simple enough that portions of the circuit (i.e., resistances) can be related to physical properties of the material. Fitting parameters and the associated errors are listed in Table 1.

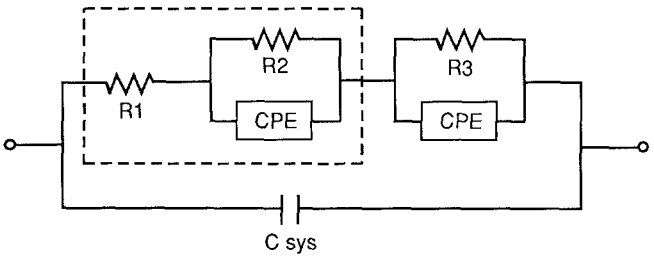

Fig. 2. The general form of the equivalent circuit used to model the overall response observed in the samples of this study. This circuit produces three impedance arcs in the complex plane, two of which can have centers below the real axis, appropriate for the polycrystalline samples. If only two impedance arcs are observed as in the single crystal experiments, the second distributed element is removed from the circuit. The portion of the circuit enclosed by the dashed box indicates the parts of the circuit that correspond solely to properties of the material. The system capacitance masks the smaller C_1 capacitance and is in parallel with the entire circuit

Single Crystal, Polycrystalline and Dunite Impedance Spectra

The most basic and direct evidence for grain boundary conduction is the comparison of the impedance spectra of a single crystal, a polycrystalline compact, and a dunite (Fig. 3). These three experiments were performed using the two-electrode technique at approximately 1200° C and similar f_{O_2}'s. In the single crystal experiment two impedance arcs are observed, while the polycrystalline compact and natural dunite display portions of three impedance arcs. The width of the first highest frequency arc for each material corresponds to a resistivity (ρ) value of 950 to 1800 Ωm. These values include differences from slightly different temperatures (1197.5–1200° C), f_{O_2}'s ($10^{-4.23}$–$10^{-5.0}$ Pa), and Fe content (Fo_{91}–Fo_{93}). At 1200° C, the expected change in resistance of the bulk mechanism from any one of these factors is less than 34% (based on T, f_{O_2}, and Fe content variations of olivine conductivity; (Schock et al. 1989; Hirsch et al. 1991; Roberts and Tyburczy 1991)). These differences do not affect the number of impedance arcs, but will have an effect on the width of the impedance arc. The resistivity values calculated from the widths of the highest frequency arcs are, however, similar to published values for the resistivity of San Carlos olivine and North Carolina dunite at similar conditions (Schock et al. 1989; Constable and Duba 1990). Thus we infer that the additional impedance arc in the polycrystalline spectra is caused by the presence of grain boundaries, and that the highest frequency impedance arc represents bulk (grain interior) conduction through the crystal.

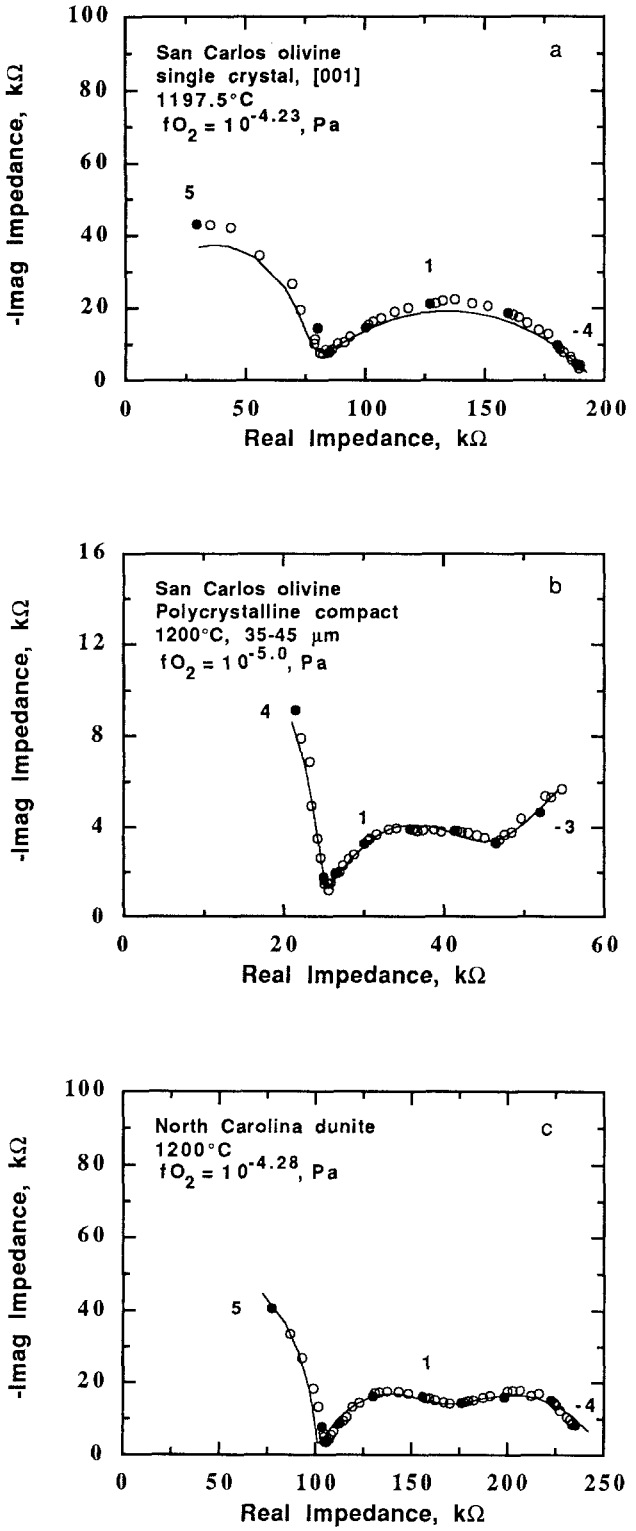

Fig. 3a, b, c. Complex impedance spectra. **a** Single crystal San Carlos olivine, 1197.5° C, $f_{O_2}=10^{-4.23}$ Pa, [001] orientation, Pt electrodes. **b** Polycrystalline San Carlos olivine compact, 1200° C, $f_{O_2}=10^{-5.0}$ Pa, 35–45 μm average grain size, Pt electrodes. **c** Dunite from Jackson County, North Carolina, 1200° C, $f_{O_2}=10^{-4.28}$ Pa, Ir electrodes. The lines through the data are models obtained by CNLS fitting with equivalent circuits

Table 2. Resistance versus l/A straight line fits

Mechanism	slope, Ωm	*y*-intercept, Ω
Polycrystalline compacts		
R1	1032±44	−3658±1533
R2	1406± 5	−13067± 143
North Carolina dunite		
R1	1752±290	6399±5877
R2	1126±106	−9301±2175

Measurements on Samples of Different Dimensions

Sato et al. (1986) measured the complex impedance of partially molten gabbro from 0.032 to 10^4 Hz using a two-electrode technique. By examining samples of constant area and different thickness they were able to evaluate the contribution of the sample electrode interface to the total impedance. They concluded that electrode polarization had no effect on the real impedance over the range of frequency measured and affected the imaginary impedance only at the lowest frequencies of measurement.

The resistance of a sample will increase for a thicker sample if the area remains constant, and will decrease for a sample of greater area if the thickness remains constant. Similarly, specific properties of a material, such as resistivity and permittivity, will remain constant for samples of varying dimensions. Properties that relate to the electrodes will vary with the area of the sample and should be independent of sample thickness. In this work we define the geometric factor (A/l) as the cross sectional area-to-thickness ratio of the sample. The resistivity is calculated from $\rho = R \cdot A/l$. where R is the resistor value determined by the curve fitting routine (Table 1). In order to compare resistances of different samples with slightly different areas, we examine the variation of resistance with the inverse of the geometric factor (l/A). When plotted in this manner, the resistance of a sample will tend to zero as the sample becomes infinitely thin and of infinite areal extent, that is, as l/A goes to zero.

In the polycrystalline samples that we have examined, the resistances of the two highest frequency mechanisms vary linearly with variation in l/A. This is shown in Fig. 4 for polycrystalline olivine compacts and a dunite from Jackson County, North Carolina. The low-frequency mechanism resistance R_3 is extremely variable. One cause of this variability is the lack of coverage of the impedance arc at the lowest frequencies, making it difficult to obtain the resistance (width) of this arc through CNLS fitting. For this reason R_3 was not plotted as a function of l/A. The polycrystalline compacts are comprised of samples with different grain sizes (Table 1). However, in polycrystalline materials such as olivine and YSZ the bulk grain boundary resistivity is independent of grain size in the grain size range of 4 to 200 μm (Verkerk et al. 1982b; Roberts and Tyburczy 1991), and the comparison is valid. The dependence of R on l/A indicates that the measured values represent

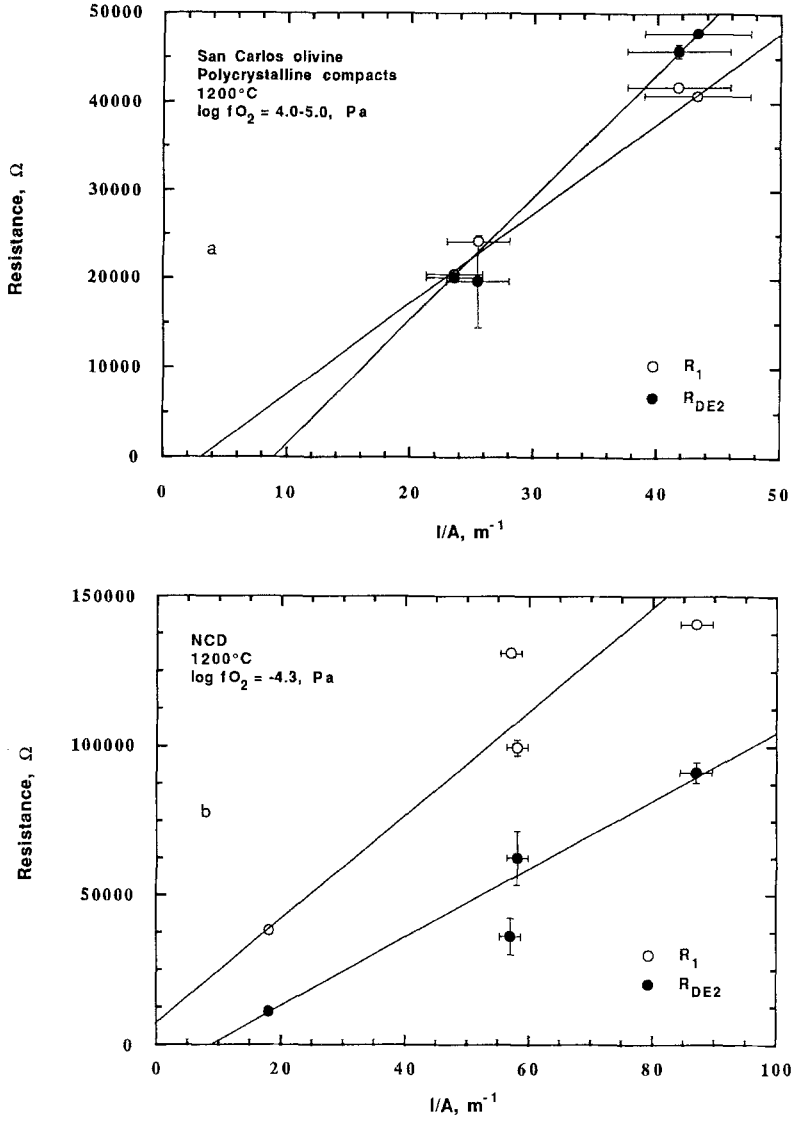

Fig. 4a, b. Resistance of the two highest frequency mechanisms plotted against the inverse of the geometric factor (l/A). *Open circles,* mechanism I (highest frequency); *filled circles* mechanism II (intermediate frequency). **a** Polycrystalline San Carlos olivine compacts, 1200° C, $f_{O_2} = 10^{-(4.0-5.0)}$. **b** North Carolina dunite, 1200° C, $f_{O_2} = 10^{-4.3}$. Lines are straight line fits, see Table 2

material properties, rather than properties of the electrodes or measurement system. The lines through the data on Fig. 4 are simple straight line fits using the equation $R = (l/A)^* a + b$, where a is the slope and b is the y-intercept. Results for these fits are shown in Table 2. One concern is the failure of these lines to have a zero intercept. There are several factors to consider including sample inhomogeneity, and temperature and f_{O_2} control. The y-intercept of R_1 for the polycrystalline compacts (Fig. 5a) using equation (6) is $-3658 \pm 1533\ \Omega$ (errors represent 1 standard deviation). The North Carolina dunites (Fig. 4b) have a y-intercept of $6399 \pm 5877\ \Omega$ for R_1. The intercepts for R_1 are not systematically positive or negative indicating that the determined resistances are not influenced by systematic errors in the measuring system or data analysis technique. The most likely reason for the non-zero intercepts is the samples are separate, physically distinct samples, and therefore may not be completely homogeneous. This is especially true for the natural samples from North Carolina. Slight differences in these samples are inevitable.

Another difficulty is the control of temperature and f_{O_2}. The temperature is accurate to within $\pm 3°$ C, and the f_{O_2} to within ± 0.15 log units. Assuming an Arrhenius type temperature dependence of the conductivity of single crystal olivine and an activation energy of 1.45 eV for conduction (Roberts and Tyburczy 1991), a temperature variation of $\pm 3°$ C for a 1200° C experiment could cause a variation in resistance measurement of $\pm 2000\ \Omega$ for a given A/l value. Similarly, if conductivity depends on f_{O_2} to the 1/5.5 power, (Schock et al. 1989), at 1200° C, an f_{O_2} variation of ± 0.15 log units has the potential for a resistance variation of $\pm 5500\ \Omega$. In spite of these potential difficulties, the resistance data in Fig. 4 do clearly demonstrate a linear dependence on sample dimension. The variation of resistance with l/A of the two highest frequency mechanisms of the polycrystalline materials is consistent with mechanisms representing properties of the materials.

Two- and Four-Electrode Experiments

Experiments performed using the four-electrode technique remove the effects of electrodes from the measure-

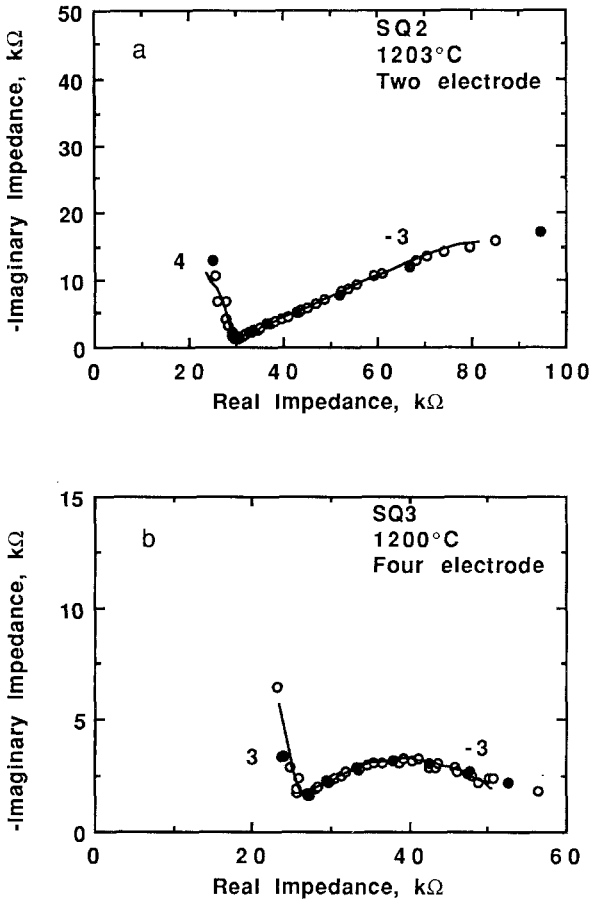

Fig. 5a, b. Complex plane plots of impedance for San Quintin dunite using two- and four-electrode methods. *Solid lines* are fits to experimental data using equivalent circuits. **a** 1203° C, two-electrode, $f_{O_2} = 10^{-5}$ Pa. **b** 1200° C, four-electrode, $f_{O_2} = 10^{-5}$ Pa. Two-electrode results show low-frequency, high impedance behavior characteristic of electrode effects. Four-electrode method eliminates electrode effects from the measurement and reveals low-frequency behavior of the sample. In the 1203° C case (a), the low frequency response of the sample is obscured by the electrode effects in the two-electrode measurement

ments (Lockner and Byerlee 1985; Olhoeft 1985). Comparison of experiments on the San Quintin dunite using two- and four-electrode configurations (Fig. 5) shows differences in both the real and imaginary parts of the impedance, particularly at low frequencies (Roberts and Tyburczy 1991). These experiments showed that one less impedance arc is present in the results using a four-electrode configuration. The remaining two impedance arcs are taken to be related to properties of the material. The two-electrode configuration experiments include a large impedance arc at the lowest frequencies of measurement that is related to electrode properties. Because of high capacitance associated with blocking at electrodes, the electrode response occurs at the lowest frequencies of measurement. Thus we conclude that the third (lowest frequency) arc represents electrical processes at the sample-electrode interface and is not related to the electrical properties of the sample, and the two highest frequency arcs represent bulk properties of the sample. These results also indicate that careful experimentation and study are required to accurately determine which portions of a particular impedance spectrum relate to sample properties as opposed to properties of the sample-electrode interface.

Comparison to Other Studies

A comparison of our results with those of similar experiments on oxide and ceramic systems (e.g., Chu and Seitz 1978; van Dijk and Burggraaf 1981; Verkerk et al. 1982a; Tuller 1985; Tanaka et al. 1987) demonstrates agreement in interpretation. When portions of three arcs are observed in these studies, they have been attributed to 1) grain interiors (highest frequency, lowest impedance arc), 2) grain boundaries (intermediate frequency and impedance arc), and 3) electrode processes (lowest frequency, highest impedance arc). Impedance arcs separated in the complex plane have time constants $\tau_1 \ll \tau_2 \ll \tau_3$, and the same trend is observed in capacitance values ($C_1 \ll C_2 \ll C_3$). If grain boundaries are a barrier to the conducting defect species and are areas where polarization occurs (Kingery et al. 1976), then it is reasonable to assume that grain boundaries have a higher capacitance than the interior of a crystal grain. Thus, a grain boundary impedance arc would occur at lower frequencies than a grain interior impedance arc.

Conclusions

Single crystal olivine and polycrystalline olivine (compacts and natural rocks) display distinctly different impedance spectra over the frequency range 10^{-4}–10^{5} Hz. The impedance spectra of polycrystalline materials exhibit two impedance arcs attributable to properties of the material, while the impedance spectra of single crystal materials display only one impedance arc related to material properties. Each impedance arc corresponds to a separate conduction mechanism that is observed over a distinct range of frequency, that is, the mechanisms add in series. Our interpretation of these mechanisms is that the highest frequency impedance arc is caused by conduction through grain interiors, and for polycrystalline materials the low-frequency impedance arc is attributable to grain boundary conduction. In both single and polycrystalline materials the impedance arc at the lowest frequencies of measurement corresponds to sample-electrode polarization effects. By modeling the electrical response with equivalent circuits of resistors and capacitors we are able to determine the separate conductivities of both grain interiors and grain boundaries. The natural dunites and the polycrystalline olivine compacts display similiar electrical behavior: the resistances of the grain interior and grain boundary mechanisms add in series. The ability to determine the separate contributions of each mechanism to the overall electrical response is dependent on the series nature of the grain interior and grain boundary mechanisms.

Acknowledgements. Bob Norton and Chris Skiba provided technical assistance. The Materials Preparation Facility at ASU assisted in the preparation of some of the samples. The computer program used in fitting the data was obtained from J.R. Macdonald. This work was supported by the National Science Foundation, Division of Earth Sciences, under grants EAR-8657357 and EAR-8916796.

References

Abelard P, Baumard JF (1980) Electric and dielectric properties of forsterite between 400 and 900° C. Phys Earth Planet Inter 23:98–102

Basu AR, Murthy VR (1977) Ancient lithospheric lherzolitic xenolith in alkali basalt from Baja California. Earth Planet Sci Lett 35:239–246

Bauerle JE (1969) Study of solid electrolyte polarization by a complex admittance method. J Phys Chem Solid 30:2657–2670

Chu SH, Seitz MA (1978) The ac electrical behavior of polycrystalline ZrO_2–CaO. J Sol St Chem 23:297–314

Constable SC, Duba AG (1990) The electrical conductivity of olivine, a dunite and the mantle. J Geophys Res 95:6967–6978

Hirsch LM, Shankland TJ (1991) Quantitative olivine defect chemical model: Insights on electrical conduction, diffusion, and the role of Fe impurities. Geophys J Int (submitted)

Hirsch LM, Shankland TJ, Duba AG (1991) Electrical conduction and mobility in Fe-bearing olivine. Geophys J Int (submitted)

Huebner JS, Voight DE (1988) Electrical conductivity of diopside: Evidence for oxygen vacancies. Am Mineral 73:1235–1254

Kingery WD, Bowen HK, Uhlmann DR (1976) Introduction to Ceramics. Wiley, New York

Kuszyk JA, Bradt RC (1973) Influence of grain size on effects of thermal expansion anisotropy in $MgTi_2O_5$. J Am Ceram Soc 56:420–423

Lockner DA, Byerlee JD (1985) Complex resistivity measurements of confined rock. J Geophys Res 90:7837–7847

Macdonald JR, Schoonman J, Lehnen AP (1982) The applicability and power of complex nonlinear least squares for the analysis of impedance and admittance data. J Electroanal Chem 131:77–95

Macdonald JR (1985) Generalizations of "universal dielectric response" and a general distribution-of-activation-energies model for dielectric and conducting systems. J Appl Phys 58:1971–1978

Olhoeft GR (1985) Low frequency electrical properties. Geophysics 50:2492–2503

Raistrick ID (1987) The electrical analogs of physical and chemical processes. In: Macdonald JR (ed) Impedance Spectroscopy. Wiley, New York, pp 27–84

Roberts JJ, Tyburczy JA (1991) Frequency dependent electrical properties of polycrystalline olivine compacts. J Geophys Res 96:16205–16222

Sato H (1986) High temperature a.c. electrical properties of olivine single crystal with varying oxygen partial pressure: implications for the point defect chemistry. Phys Earth Planet Inter 41:269–282

Sato H, Manghnani MH, Lienert BR, Weiner AT (1986) Effects of electrode polarization on the electrical properties of partially molten rock. J Geophys Res 91:9325–9332

Schock RN, Duba AG, Shankland TJ (1989) Electrical conduction in olivine. J Geophys Res 94:5829–5839

Tanaka J, Baumard J, Abelard P (1987) Nonlinear electrical properties of grain boundaries in an oxygen-ion conductor ($CeO_2 \cdot Y_2O_3$). J Am Ceram Soc 70:637–643

Tuller HL (1985) Electrical conduction in ceramics: Toward improved defect interpretation. In Schock RN (ed) Point Defects in Minerals, Geophysical Monograph 31:47–68, American Geophysical Union, Washington, D.C.

Tyburczy JA, Roberts JJ (1990) Low frequency electrical response of polycrystalline olivine compacts: Grain boundary transport. Geophys Res Lett 17:1985–1988

van Dijk T, Burggraaf AJ (1981) Grain boundary effects on ionic conductivity in ceramic Gd × Zr1-xO2-(x/2) solid solutions. Phys Status Solidi 63:229–240

Verkerk MJ, Winnubst AJA, Burggraaf AJ (1982a) Effect of impurities on sintering and conductivity of yttria-stabilized zirconia. J Mat Sci 17:3113–3122

Verkerk MJ, Middelhuis BJ, Burggraaf AJ a(1982b) Effect of grain boundaries on the conductivity of high-purity ZrO2-Y2O3 ceramics. Solid State Ion 6:159–170